INTERNATIONAL ATOMIC ENERGY AGENCY
UNITED NATIONS EDUCATIONAL, SCIENTIFIC AND CULTURAL ORGANIZATION
INTERNATIONAL CENTRE FOR THEORETICAL PHYSICS
I.C.T.P., P.O. BOX 586, 34100 TRIESTE, ITALY, CABLE: CENTRATOM TRIESTE

H4.SMR/841-13

FOURTH ICTP-URSI-ITU(BDT) COLLEGE ON RADIOPROPAGATION:
Propagation, Informatics and Radiocommunication System Planning

30 January - 3 March 1995

Miramare - Trieste, Italy

The Application of Radio Propagation Studies to System Planning

L. Barclay
Barclay Associates Ltd.,
Chelmsford, United Kingdom

The Application of Radio Propagation Studies to Sytem Planning

Les Barclay
Barclay Associates Ltd.
fax: +44 1621 828539

The information society

expanding demand for
- information
- telecommunications

bandwidth provided by

cable

optical fibres

demand for

mobility

flexibility

low costs

met by Radiocommunications

but radio usage limited by the e.m. spectrum

need to share frequencies
coordinate usage
regulate

- improve utilisation of the spectrum
- improve techniques for frequency sharing
- evaluate potential of new technology & its impact on spectrum demand
- design of modems, coding schemes and antennas
- specification of equipment parameters
  - relating to quality of transmission & emc leading to system and equipment standards

CURRENT TOPICS

millimetric wavelengths

interference (UHF and SHF)

diffraction and scatter

earth/space

digital systems

mobile systems

HF propagation

VHF - SHF propagation considerations

Reflection

Diffraction

Refraction

Scatter

isotropic radiator in free space

$$s = \frac{p_t}{4\pi d^2}$$

$$s = \frac{e^2}{120\pi}$$

$$e = \frac{\sqrt{30 p_t}}{d}$$

$\lambda/2$ dipole

$$e = \frac{\sqrt{1.65 \times 30 p_t}}{d}$$

$$e \approx 7\frac{\sqrt{p_t}}{d}$$

$$E = 107 + \underset{dB(kW)}{P_t} - 20 \log \underset{km}{d} \quad dB(\mu$$

The impedance of free space is $120\pi\ \Omega$.

field strength

$$e = \sqrt{S . Z_0}$$

$$= \sqrt{\frac{P_t}{4\pi d^2} . 120\pi}$$

$$= \frac{\sqrt{30 . P_t}}{d}$$

$\approx 173\ mV/m$ [For 1kW, at 1km]

2

effective aperture of isotropic receiving antenna is $\frac{\lambda^2}{4\pi}$

received power (power available in a matched load)

$$P_r = S . A$$

$$= \frac{P_t}{4\pi d^2} . \frac{\lambda^2}{4\pi}$$

i.e. $\frac{P_r}{P_t} = \left(\frac{\lambda}{4\pi d}\right)^2$

Free space basic transmission loss

$$L_{bf} = 10 \log\left(\frac{P_t}{P_r}\right) = 20 \log\left(\frac{4\pi d}{\lambda}\right)$$

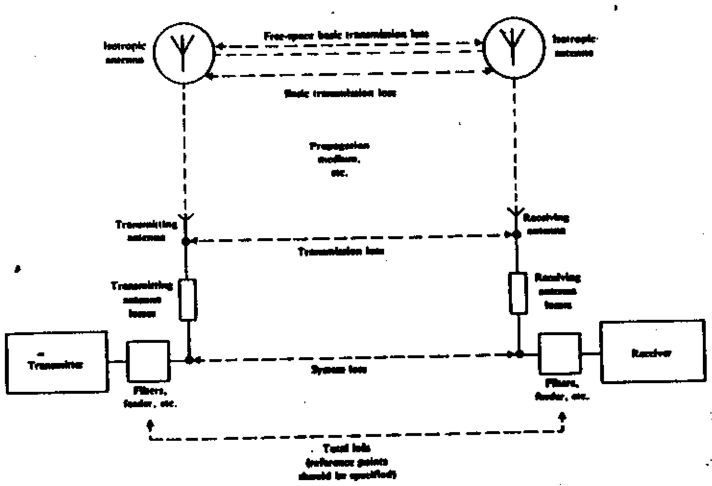

FIGURE 1 – Graphical depiction of terms used in the transmission loss concept

Complex Relative Permittivity

$$\varepsilon_r^* = \varepsilon_r - j\frac{\sigma}{\omega\varepsilon_o} = \varepsilon_r - j60\sigma\lambda$$

Relative permittivity, ε_r, and conductivity, σ, as a function of frequency

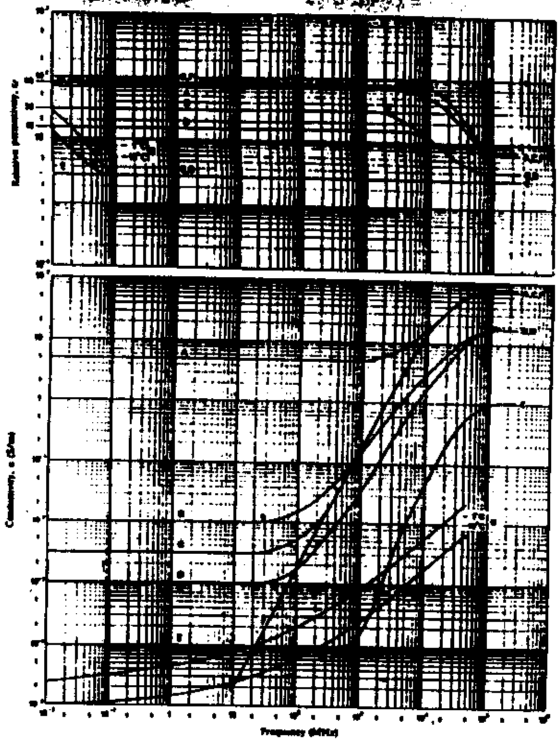

A: sea water (average salinity), 20°C
B: wet ground
C: fresh water, 20°C
D: medium dry ground
E: very dry ground
F: pure water, 20°C
G: ice (fresh water)

REFLECTION COEFFICIENT

horizontal polarisation

$$R_H = \frac{\sin\phi - \left(\varepsilon_r^* - \cos^2\phi\right)^{0.5}}{\sin\phi + \left(\varepsilon_r^* - \cos^2\phi\right)^{0.5}}$$

vertical polarisation

$$R_V = \frac{\varepsilon_r^*\sin\phi - \left(\varepsilon_r^* - \cos^2\phi\right)^{0.5}}{\varepsilon_r^*\sin\phi + \left(\varepsilon_r^* - \cos^2\phi\right)^{0.5}}$$

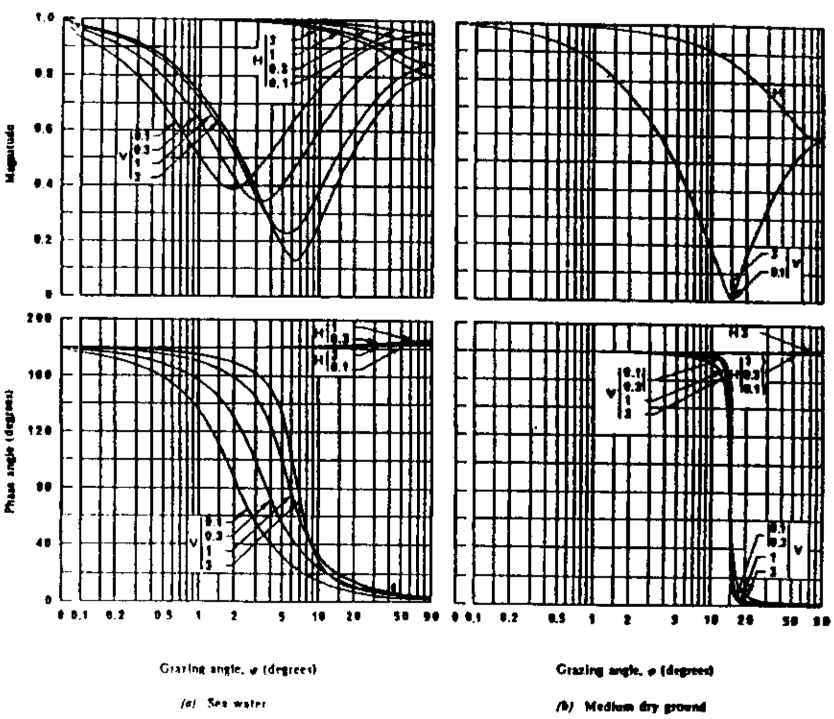

Magnitude and phase of the reflection coefficient of a plane surface as functions of grazing angle, ψ, for vertical V and horizontal H polarizations

The frequencies are given in GHz

Consider two elevated antennas with a smooth, plane earth

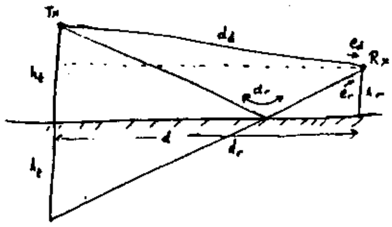

$$d_d = \left[d^2 + (h_t - h_r)^2\right]^{1/2} \approx d\left[1 + \tfrac{1}{2}\left(\frac{h_t - h_r}{d}\right)^2\right]$$

$$d_r = \left[d^2 + (h_t + h_r)^2\right]^{1/2} \approx d\left[1 + \tfrac{1}{2}\left(\frac{h_t + h_r}{d}\right)^2\right]$$

thus $\quad d_r - d_d = \dfrac{2h_t h_r}{d}$

this path difference gives a phase difference

$$\phi = \frac{2\pi}{\lambda} \cdot \frac{2h_t h_r}{d} = \frac{4\pi h_t h_r}{\lambda d} \quad \text{radians}$$

When $e_d = -e_r$. (a reflection coefficient of -1)

the resultant field is

$$|e_t| = \left|2\, e_d \sin\left(\frac{2\pi h_t h_r}{\lambda d}\right)\right|$$

In terms of the cymomotive force e_1

$$|e_t| = \left|2\,\frac{e_1}{d} \sin\left(\frac{2\pi\, h_t h_r}{\lambda d}\right)\right|$$

[cmf is the product field strength and distance in a lossless situation. i.e. e_1 is the field strength at 1km, when d is in km

In logarithmic terms

$$E_t = 6 + E_1 - 20\log d\,(\text{km}) + 20\log\left[\sin\frac{2\pi h_t h_r}{\lambda d}\right]$$

i.e it has the usual $20\log d$ distance term

modified to be 6dB greater when

$\dfrac{2\pi h_t h_r}{\lambda d} = \dfrac{k\pi}{2}$ and K is an odd integer

and reducing to zero amplitude $[-\infty\, \text{dB}]$ (theoretically!) when K is an even integer

5 - 7

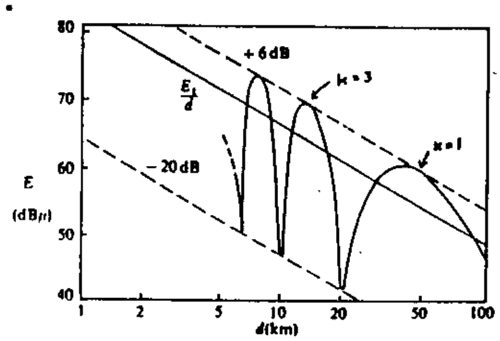

Variation of field strength with distance including a reflected ray ($\rho = -1$)

at distances beyond $k = 1$,

i.e. when $\dfrac{2\pi\, h_t h_r}{\lambda d}$ is small

$$|e_t| \approx 2\,\frac{e_1}{d} \cdot \frac{2\pi h_t h_r}{\lambda d}$$

$$\text{i.e.}\quad e_t \propto \frac{1}{d^2}$$

giving 40dB decrease for a 10 times increase with distance.

5-Ray Reflection Model: Fig. 1

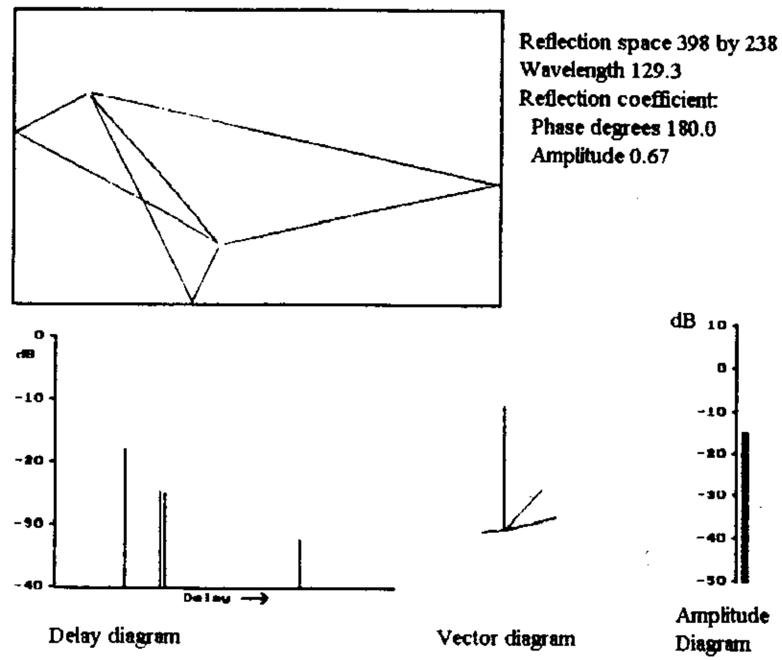

The Delay Diagram plots the amplitude of each component at the receiver against the time delay due to different path pengths.

The Vector Diagram plots the amplitude and phase of each component at the receiver, with the direct ray normalised to unity and zero phase angle (vertical).

The Amplitude Diagram gives the amplitude of the vector sum of the five rays at the receiver.

5-Ray Reflection Model: Fig. 3

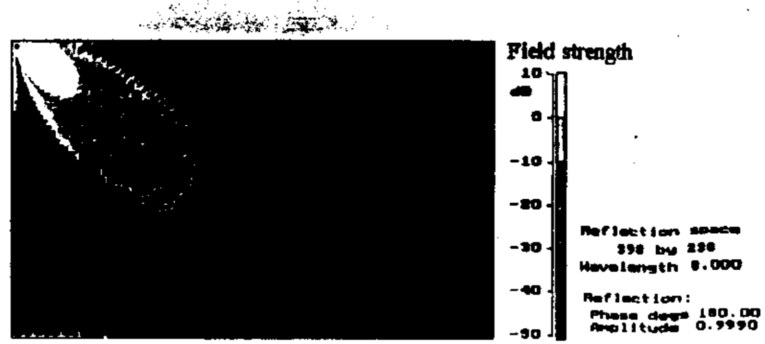

Wavelength is short compared to size of room.
Reflection coefficient = -1

The transmitter is close to the top-left corner, such that the direct ray and the reflections in both the left and top walls all reinforce to form a beam which remains well defined in the vicinity of the transmitter, where the other two rays are relatively small. Further from the transmitter all five rays are comparable, producing an interference pattern.

4. DIFFRACTION

However radiowaves will also diffract around and behind obstacles.

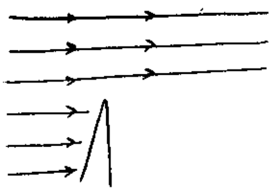

This cannot be explained by simple ray models.

The field strength beyond a knifeedge is given by:

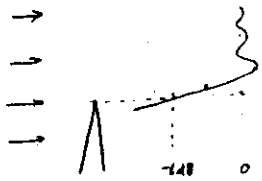

a 6dB reduction exactly on the geometric shadow line with ripples in the visible region and an ~~exponential~~ continuous decrease in the shadow

Huygens proposed that each point on a wavefront should be considered as the source of a spherical "wavelet". The envelope of these gives the new wavefront.

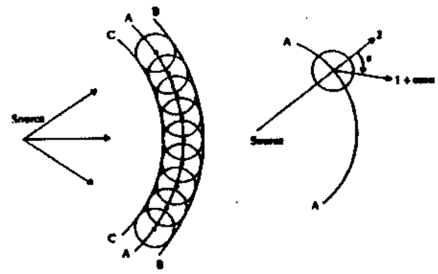

Huygens' principle applied to a spherical wavefront.

Thus for a plane wave front meeting a knife-edge obstruction

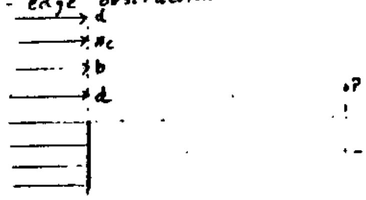

The field strength at P may be found by a vector addition of the components from wavelets a, b, c, d, -- etc.

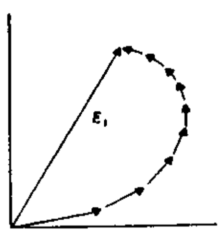

The change in phase is due to the increasing length of the ray path from successive 'wavelet' sources.

This leads to the Cornu spiral for a plane wave field incident at a knife edge. The spiral is normalised in terms of a parameter, ν.

$$\nu = s\sqrt{\frac{2}{\lambda}\left(\frac{1}{d_1} + \frac{1}{d_2}\right)}$$

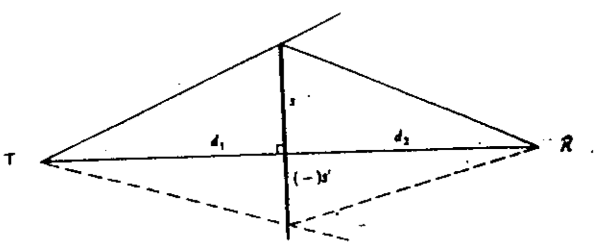

The geometry of diffraction.

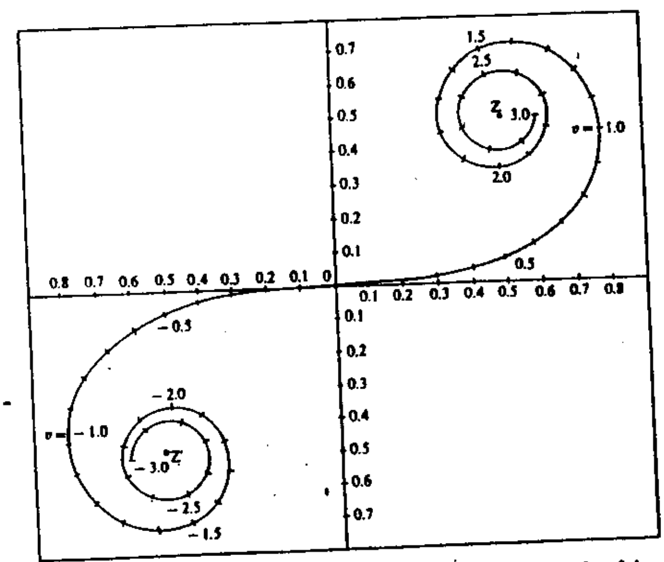

Cornu's spiral for diffraction over a knife-edge obstacle. It is a plot of the Fresnel's integrals in terms of the auxiliary parameter v.

When part of the wavefront is obstructed, the field may be found by finding the resultant of the unobstructed part of the spiral.

Knife-edge diffraction loss

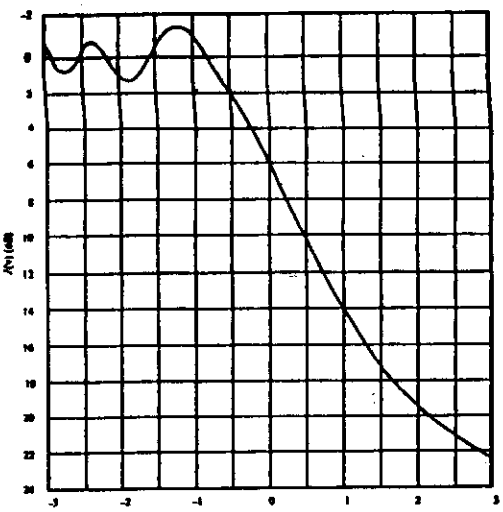

at the geometrical shadow line ($\nu = 0$) there is a 6dB loss.

There is a ripple in the illuminated zone.

The loss well into the shadow zone may be approximated : $20 \log \frac{0.225}{\nu}$ dB

For double knife edges, the loss is computed for each, with a part path length from the other edge to the nearer terminal.

Method for double isolated edges

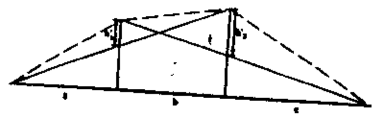

This may be extended to multiple knife edges.

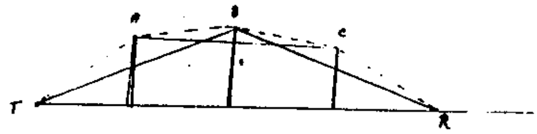

Note that earlier methods, which found a synthetic single edge, are WRONG

5-17

Ensuring that the k=1 ellipsoid does not contain obstructions gives <u>Fresnel zone clearance</u>.

It is sufficient to ensure clearance of 0.6 of the first Fresnel zone (see viewfoil 5-15)

To establish a good reflection, the whole of the first Fresnel zone for reflection must be available

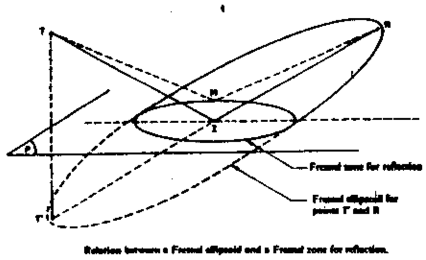

Relation between a Fresnel ellipsoid and a Fresnel zone for reflection.

5-16

This concept leads to the idea of the zone-plate where annular obstructions cut-out out of phase contributions.

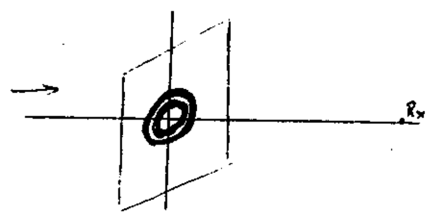

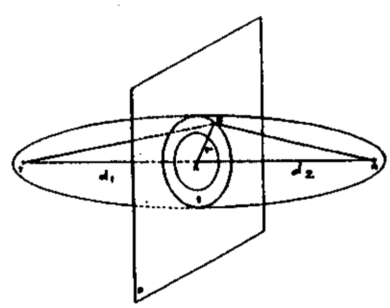

Fresnel ellipsoid, a surface of constant phase difference

$$r^2 = k\lambda\left(\frac{d_1 d_2}{d_1 + d_2}\right)$$

- **Diffraction over a transhorizon path**

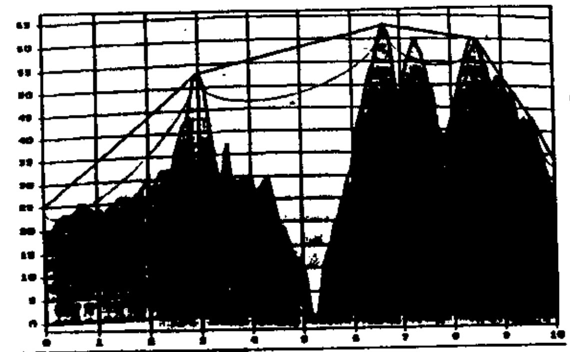

However, in real circumstances, most obstructions are rounded, and the path may be modelled by fitting cylinders to each hill top.

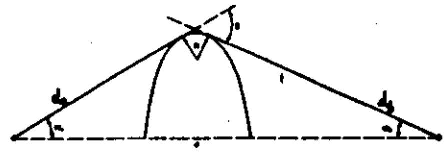

Rounded hills give substantially greater losses given by:

$$A = J(\nu) + T(\rho) + Q(\chi)$$

$J(\nu)$ is the knife edge loss as described earlier for the parameters used in the above diagram

$$\nu = 2\sin\frac{\theta}{2}\cdot\left[\frac{2(d_a + R\,\theta/2)(d_b + R\,\theta/2)}{\lambda d}\right]^{1/2}$$

$T(\rho)$ is the loss for incidence upon the curved surface given by.

$$T(\rho) = 7.2\rho - 2\rho^2 + 3.6\rho^3 - 0.8\rho^4$$

where $\rho = \dfrac{d_a + d_b}{d_a d_b} \Big/ \left[\left(\dfrac{\pi R}{\lambda}\right)^{1/3}\cdot\dfrac{1}{R}\right]$

and $Q(\chi)$, the loss for propagation along the curved surface between horizons is given by.

$$Q(\chi) = \begin{cases} T(\rho)\,\chi/\rho & \text{for } -\rho \le \chi < 0 \\ 12.5\,\chi & \text{for } 0 \le \chi < 4 \\ 17\chi - 6 - 20\log\chi & \text{for } \chi \ge 4 \end{cases}$$

where $\chi = \left(\dfrac{\pi R}{\lambda}\right)^{1/3}\theta$

$$\approx \sqrt{\frac{\pi}{2}}\,\nu\rho \quad \text{if } \theta \ll 1$$

For multiple rounded hills a technique similar to that for knife edges is used.

The cascaded cylinder model a) overall problem, b) details

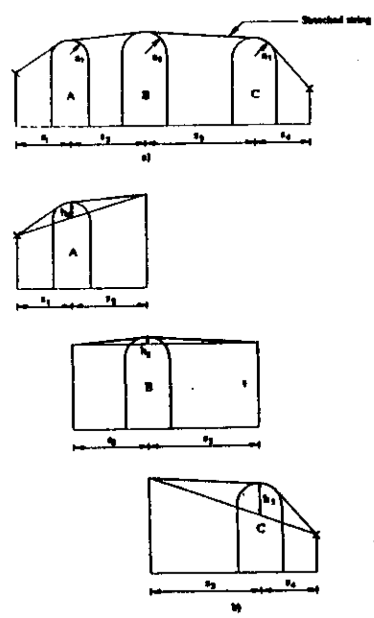

REFRACTION

The refractive index of air at the earth's surface is very close to unity. For practical purposes a refractivity unit is used.

$$N = (n-1)10^6 = 77.6\frac{P}{T} + 3.73\times10^5\frac{e}{T^2}$$

- n is the refractive index
- P is the pressure (hPa or mb)
- T temperature (K)
- e water vapour pressure (hPa or mb)

In equilibrium, the refractivity varies exponentially with height

$$N = N_s\, e^{-z/Z}$$

where N_s is the value at the surface
z is the height
and Z is the scale height

The ITU-R reference atmosphere has

$N_s = 315$

$Z = 7.35$ km

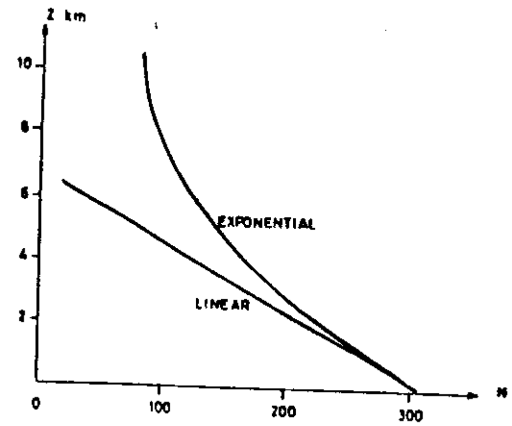

In the first kilometre it is sufficient to assume a linear variation of N; about 40 N units per km

$$N \approx 315 - 40h$$

For a horizontally stratified medium with varying refractivity, the rays are bent according to Snell's law.

$$n_x \sin i_x = \text{constant}$$

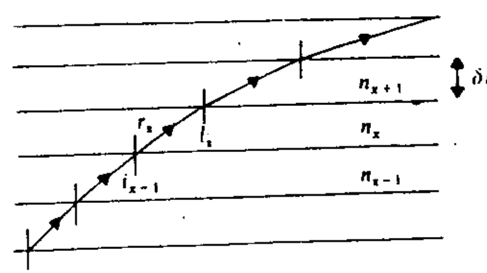

6- 3

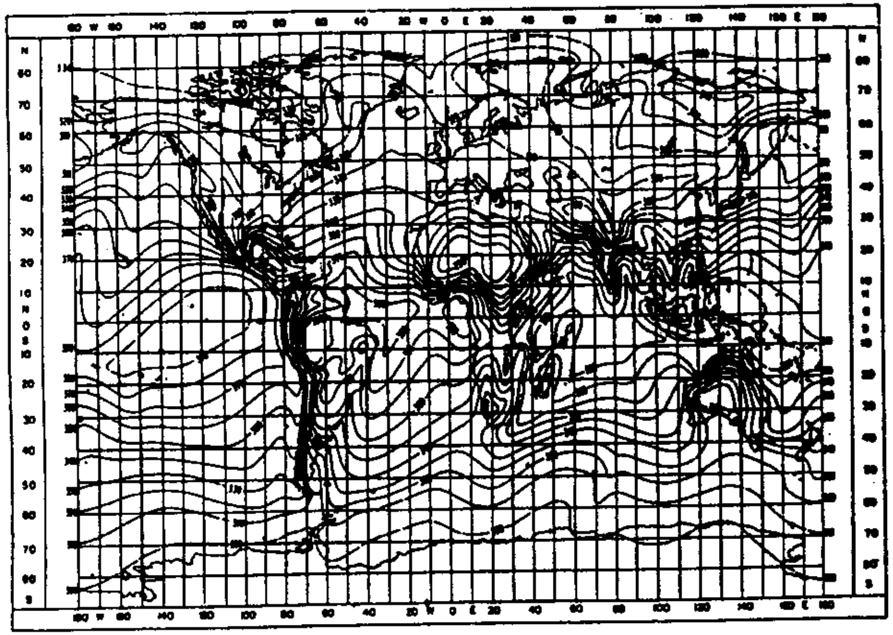

– World-wide mean value of N_s: February

6-4

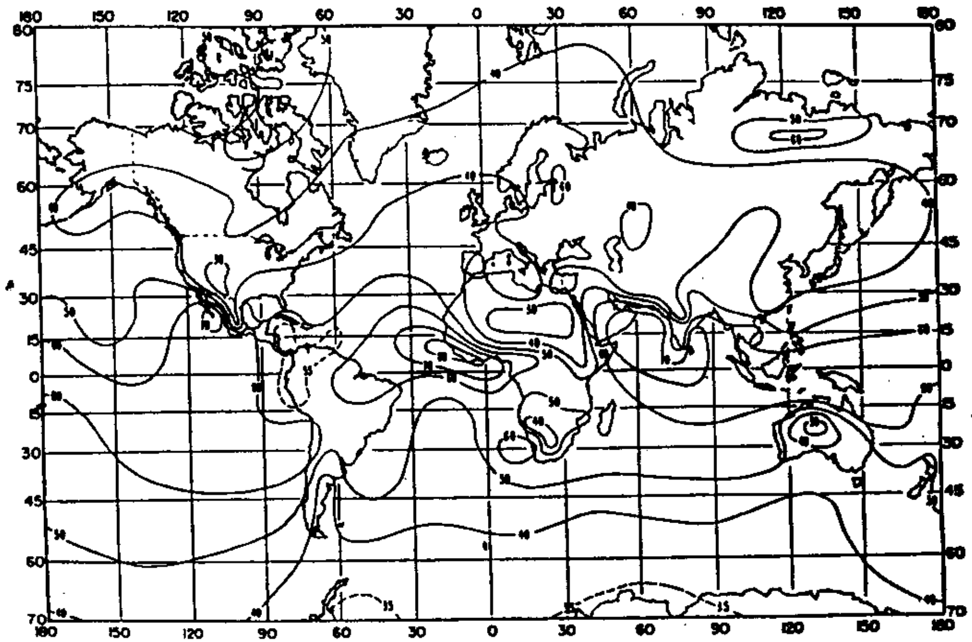

– Monthly mean values of ΔN: February

11

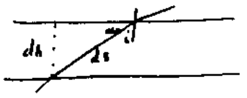

$dh = ds \cdot \sin\alpha$

$\sin i_x \cdot n = C = \cos\alpha_x \cdot n$

$\cos\alpha_x \dfrac{dn}{ds} - n \sin\alpha_x \dfrac{d\alpha_x}{ds} = 0$

$\dfrac{d\alpha_x}{ds} = \dfrac{\cos\alpha_x}{n \sin\alpha} \dfrac{dn}{ds} = \dfrac{\cos\alpha_x}{n} \dfrac{dn}{dh}$

The radius of curvature is thus:

$R_x = \dfrac{n}{\cos\alpha_x \cdot dn/dh}$

For rays which are nearly horizontal

$R_x \approx 25{,}000$ km

The radius of the earth

$R_e = 6371$ km

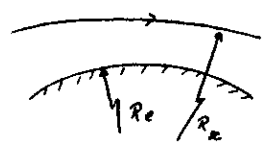

For convenience, we make a geometrical transformation to make either the ray path, or the earth's surface, flat.

$\dfrac{1}{R_x} = \dfrac{1}{25{,}000} = 40 \times 10^{-6}$

$\dfrac{1}{R_e} = \dfrac{1}{6{,}371} = 157 \times 10^{-6}$

Reducing both curvatures by 40×10^{-6}:

- the propagation path will have zero curvature
- the effective earth ~~radius is~~ curvature is

$(157 - 40) \times 10^{-6} = 117 \times 10^{-6}$

i.e. the effective radius is 8547 km

$\approx 4/3\, R_e$

6-8

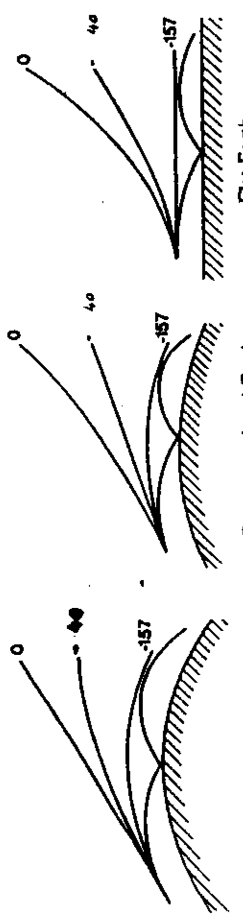

Fig. 4.8. Various representations of a path starting in a horizontal direction. Parameter: three particular values of the refractive index gradient.

6-7

Alternatively, if the earth is flattened, the ray has an upward curvature of 117×10^{-6}.

This may be achieved mathematically by modifying the refractivity

$M = 315 + 117h$

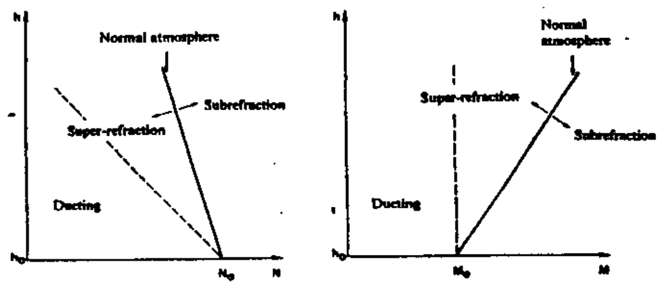

The different refraction conditions in the atmosphere.

6-9

One way to model changes in the refractivity on a statistical basis is to adjust the effective earth's radius used in the ray-path analysis

- e.g. to determine whether the path has Fresnel zone clearance.

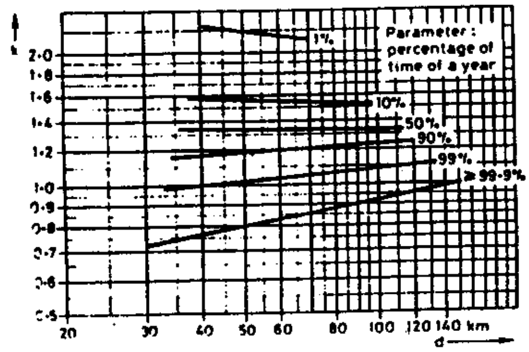

6-10

However, stratification in the atmosphere can lead to substantial departures from an exponential decrease of N with height.

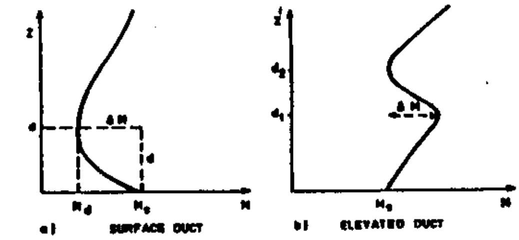

6-11

Types of ducting

- evaporation
  - surface duct over sea
    - due to decrease in humidity with height
- advection
  - surface duct over colder (e.g. sea)
    - due to winds blowing from warmer surface
- subsidence inversion
  - elevated duct in anticyclonic area
    - due to slow settling of air from high level
    - the high air is warmer and drier
- radiation inversion
  - surface duct
    - due to radiative cooling of surface after sunset
- fronts
  - complex refractivity changes

6-12

evaporation duct

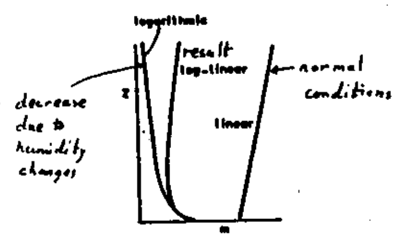

Components of m in an evaporation duct

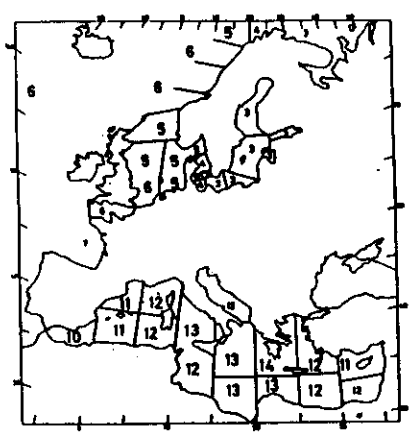

mean evaporation duct thickness

6-14

6-15

- ray paths in ducts

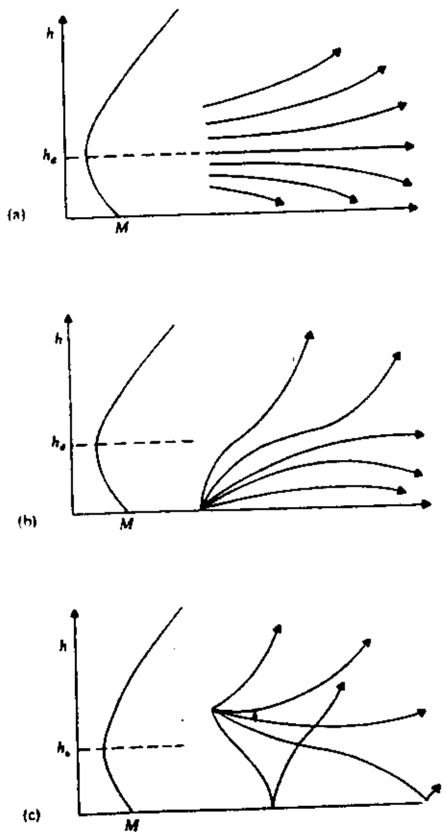

Fig. 4.16 The effect of modified refractive index on (a) horizontally propagating waves at different heights, (b) waves emanating from a low antenna, and (c) waves emanating from an elevated antenna. The variation of M with height indicates a surface duct.

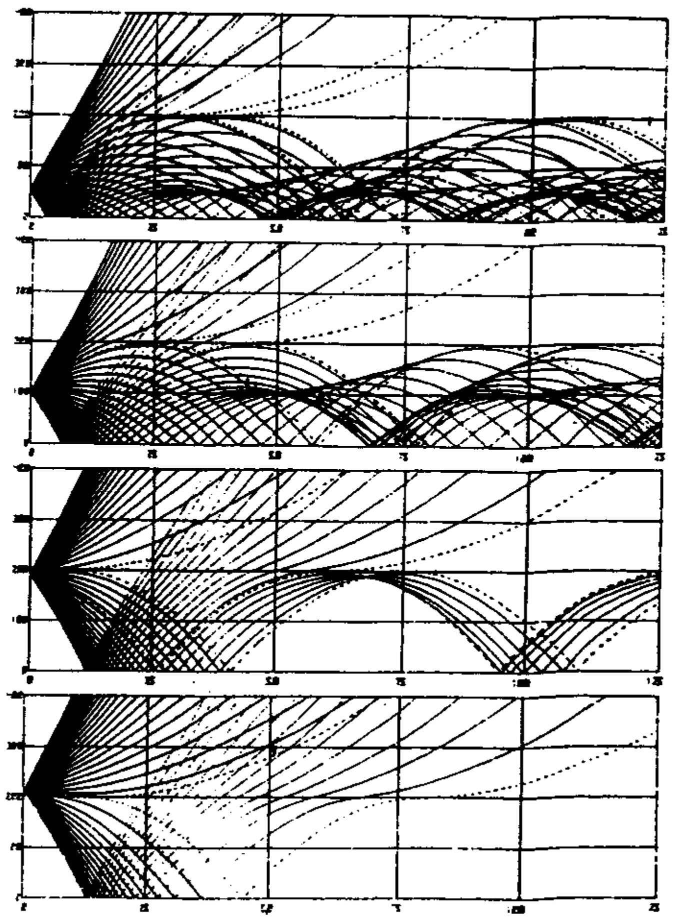

Path forms: Refractive index gradient in the duct: −500N/km. Thickness of the duct: 200m. Height of transmitter: 50m; 100m; 190m; 210m.

14

millimetric wavelengths

vast spectrum

- many new communication opportunities
- high data rates

limited range

- - - - - - - - - - - - - - - - - -

point to multipoint - MVDS
wireless infrastructure for microcellular systems
cordless office (wireless LANs)
telemetry
road transport - collaborative driving

earth/space

GEO:
rain attenuation
depolarization
mm wavelengths

non GEO:
UHF
scintillation
high angle propagation
into urban areas and trees

interference - UHF & SHF

terrestrial & earth/space

availability and reliability

coordination procedures

detailed predictions

- radio meteorology
- rain scatter
- topography
- coastal regions

digital systems

microwave "line of sight" trunks

digital speech and vision

data

. . . .

spread spectrum (CDMA)
multi-level QAM
coding

what are the required parameters?

MOBILE and BROADCASTING

diffraction, reflection, scatter

digital

terrestrial and earth/space

now up to 2GHz - will go higher

. . . .

microcellular
within building
DAB

terrestrial/satellite cellular systems interface

AREA COVERAGE

Both broadcasting and mobile communications have to ensure reliable communication between a fixed base-station and stations anywhere within an area.

For VHF and UHF television broadcasting, predictions are generally made:

- for a receiving antenna height of 10m
- for 50 or 90% of locations
- for 90, 95 or 99% of the time.

A long established ITU-R method (Rec 370) provides curves of field strength for the above conditions and for land, cold seas and warm seas.

In this method

- the height of the transmitting antenna is taken as the height above average terrain between 3 and 15 km from transmitter.
- the height of the receiving antenna is taken as 10m above local terrain.
- a terrain roughness parameter Δh is determined.

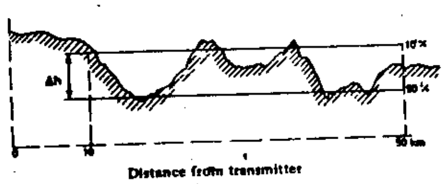

– Application of the parameter Δh for broadcasting services

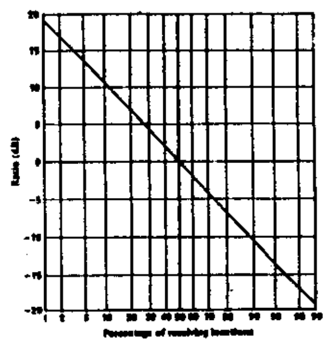

– Ratio (dB) of the field strength for a given percentage of the receiving locations to the field strength for 50% of the receiving locations

Frequency: 30 to 250 MHz (Bands I, II and III)

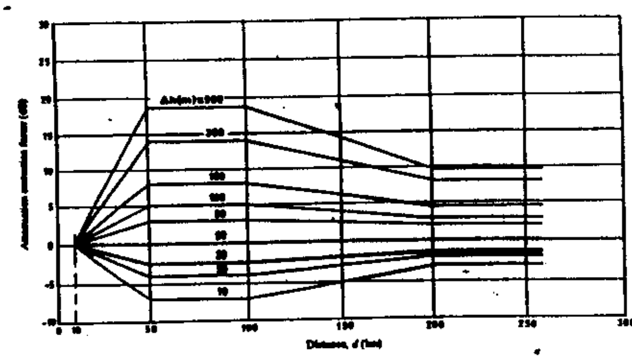

– Attenuation correction factor as a function of the distance d (km) and Δh

Frequencies 80 to 250 MHz (Bands II and III)

18-5

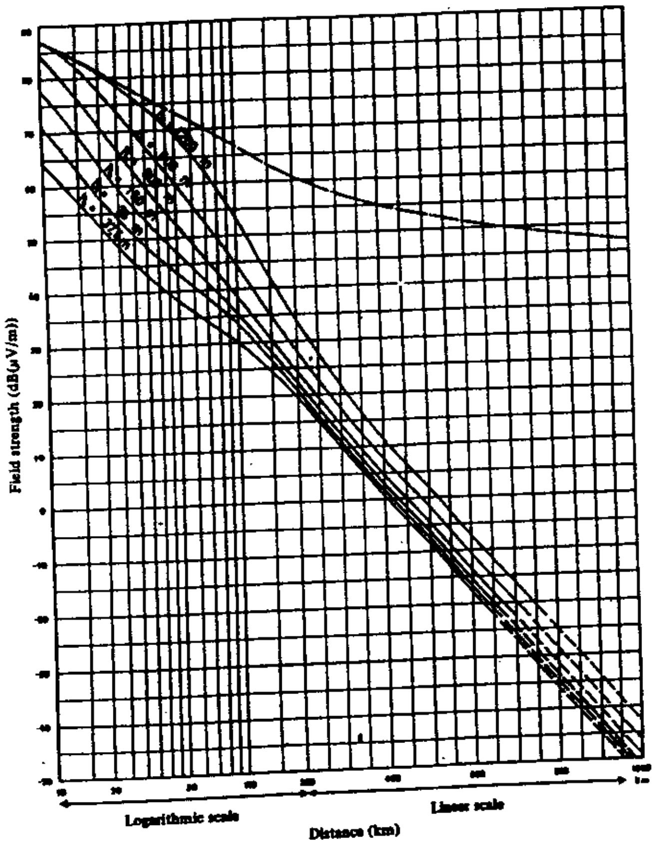

– Field strength (dB(μV/m)) for 1 kW e.r.p.

Frequency: 30 to 250 MHz (Bands I, II and III) - Land - 1% of the time - 50% of the locations - h_2 = 10 m - Δh = 50 m

—·— Free space

VHF, Land, 1%

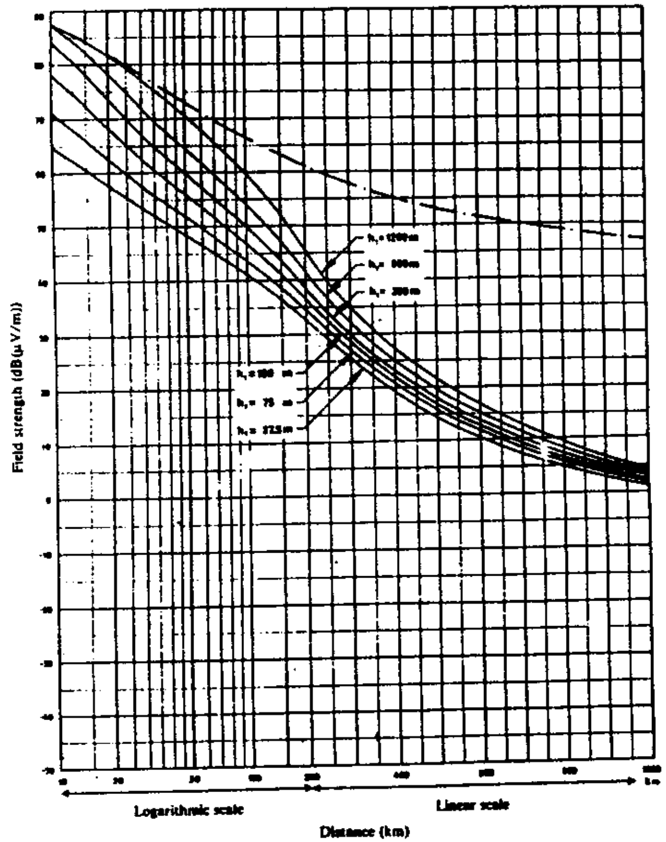

– Field strength (dB(μV/m)) for 1 kW e.r.p.

Frequency: 30 to 250 MHz (Bands I, II and III) - Warm sea (excluding areas subject to extreme super-refraction) - 1% of the time - 50% of the locations - h_2 = 10 m

—·— Free space

VHF, warm sea, 1%

3-7

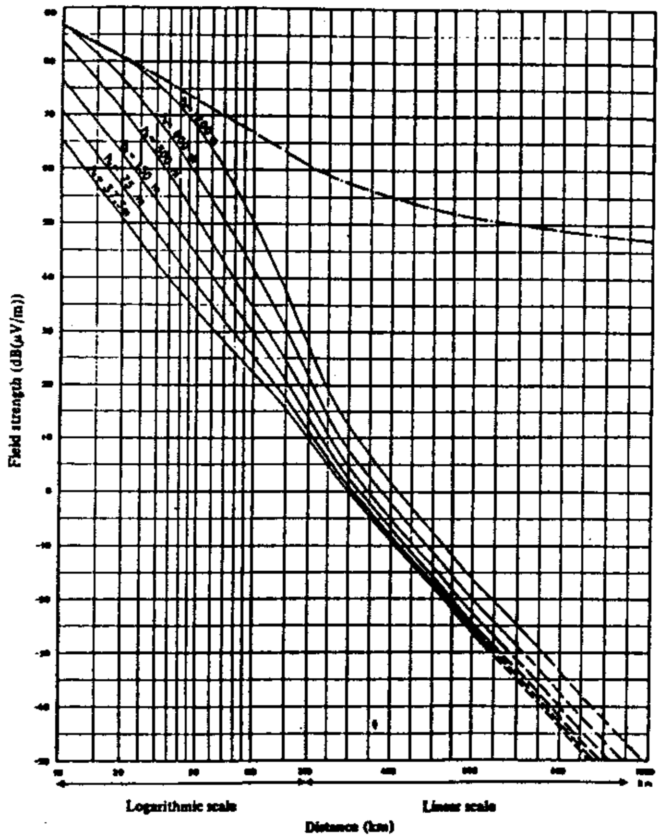

– Field strength (dB(μV/m)) for 1 kW e.r.p.

Frequency: 450 to 1000 MHz (Bands IV and V) – Land – 1% of the time – 50% of the locations – $h_2 = 10$ m – $\Delta h = 50$ m

—·— Free space

3-X

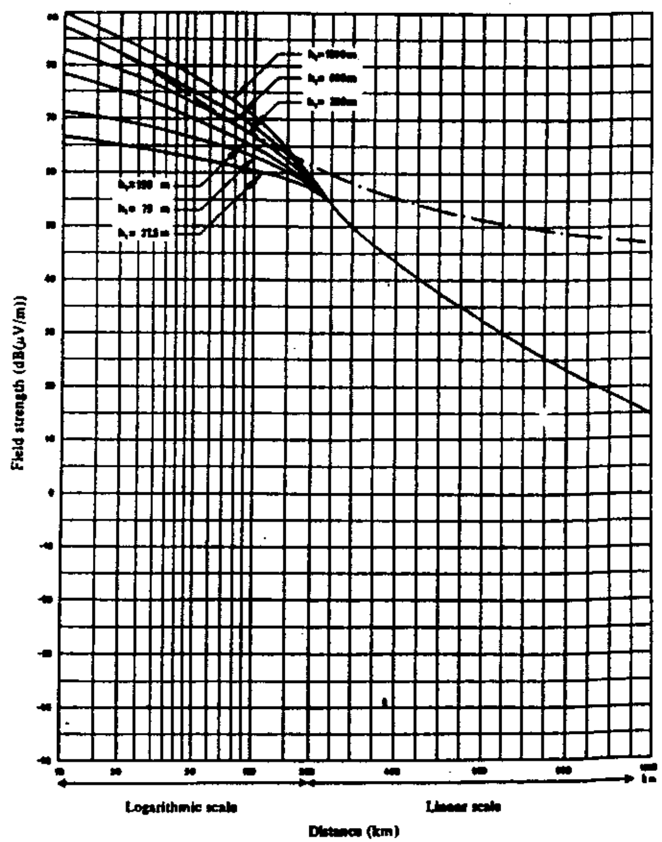

– Field strength (dB(μV/m)) for 1 kW e.r.p.

Frequency: 450 to 1000 MHz (Bands IV and V) – Warm sea (excluding areas subject to extreme super-refraction) – 1% of the time – 50% of the locations – $h_2 = 10$ m

—·— Free space

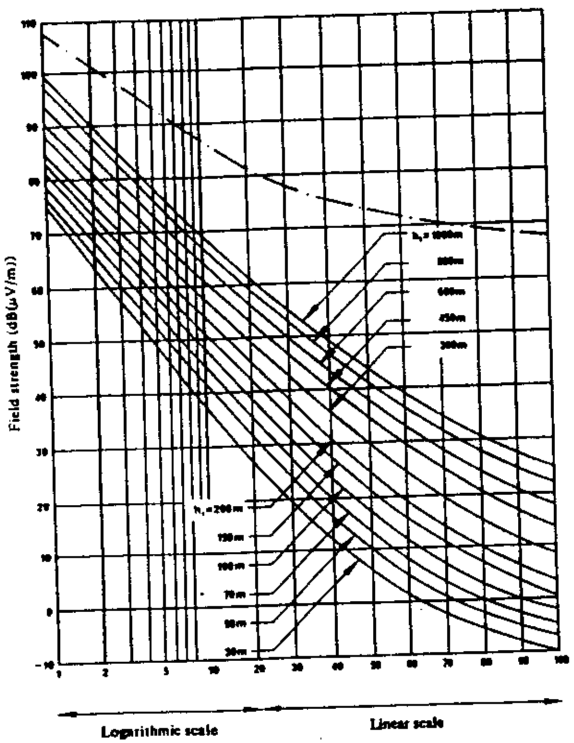

FIGURE 2 – Field strength (dB(μV/m)) for 1 kW e.r.p.

Frequency ≈ 900 MHz, urban area 50% of the time; 50% of the locations; $h_r = 1.5$ m

—·—·— Free space

13-15

Okumura's method. 100 - 3000 MHz

urban, Tokyo

Hata's formulation

In an attempt to make the Okumura method easy to apply, Hata [15] established empirical mathematical relationships to describe the graphical information given by Okumura. Hata's formulation is limited to certain ranges of input parameters and is applicable only over quasi-smooth terrain. The mathematical expressions and their range of applicability are:

Urban areas

$$L_{50} = 69.55 + 26.16 \log f_c - 13.82 \log h_t - a(h_r) + (44.9 - 6.55 \log h_t) \log d \quad \text{dB} \tag{4.6}$$

where

$$150 \leqslant f_c \leqslant 1500 \quad (f_c \text{ in MHz})$$
$$30 \leqslant h_t \leqslant 200 \quad (h_t \text{ in m})$$
$$1 \leqslant d \leqslant 20 \quad (d \text{ in km})$$

$a(h_r)$ is the correction factor for mobile antenna height and is computed as follows:

For a small or medium-sized city,

$$a(h_r) = (1.1 \log f_c - 0.7)h_r - (1.56 \log f_c - 0.8) \tag{4.7}$$

where $1 \leqslant h_r \leqslant 10$ m.

For a large city,

$$a(h_r) = \begin{cases} 8.29(\log 1.54h_r)^2 - 1.1 & : f \leqslant 200\,\text{MHz} \\ 3.2(\log 11.75h_r)^2 - 4.97 & : f \geqslant 400\,\text{MHz} \end{cases} \tag{4.8}$$

Suburban areas:

$$L_{50} = L_{50}(\text{urban}) - 2[\log(f_c/28)]^2 - 5.4 \quad \text{dB} \tag{4.9}$$

Open areas:

$$L_{50} = L_{50}(\text{urban}) - 4.78(\log f_c)^2 - 18.33 \log f_c - 40.94 \quad \text{dB} \tag{4.10}$$

Specific attenuation of woodland

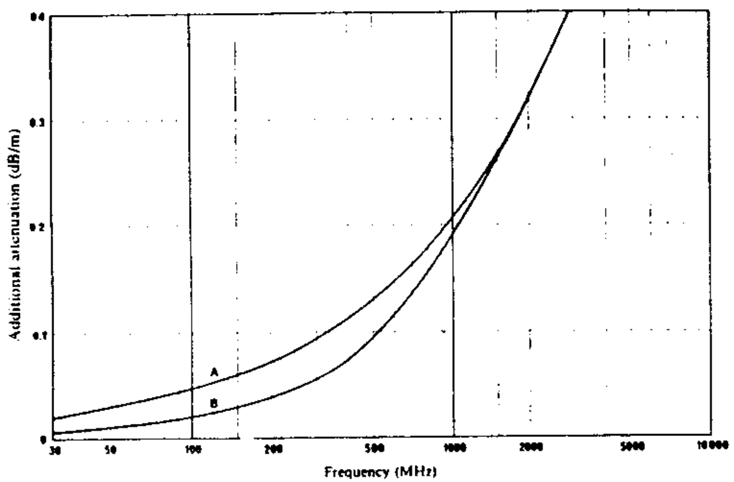

A: vertical polarization
B: horizontal polarization

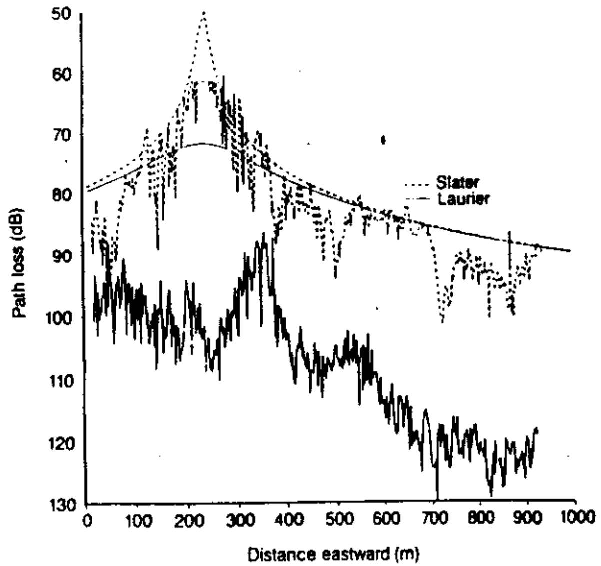

Fig. 4.21 Path loss measurements at 910 MHz along two parallel streets in Ottawa, Canada; (vertical lines indicate street crossings, smooth curves show calculated free-space loss)

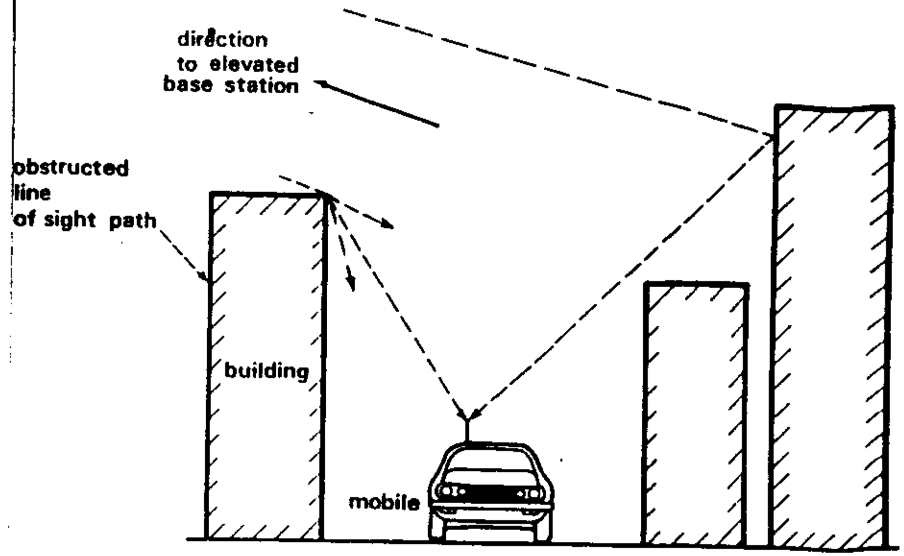

Illustrating the mechanism of radio propagation in urban areas

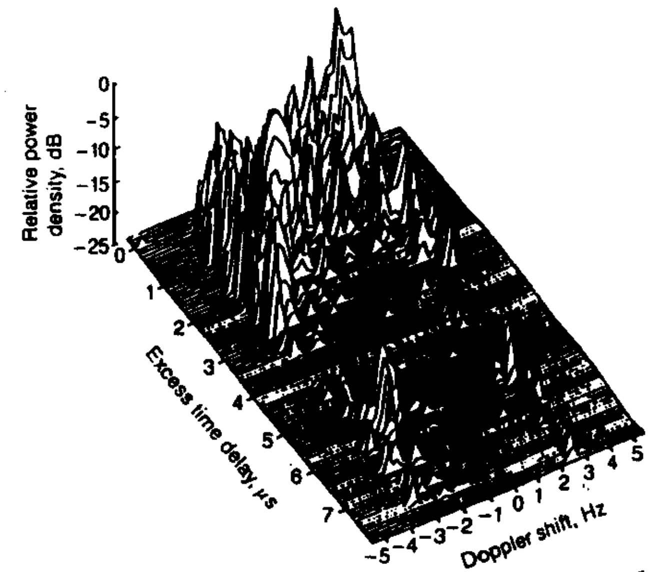

Example of a scattering function in a severe multipath area

COVERAGE PREDICTION 1.4C

Centre = TQ300800
Map is 90.0 km on the side
Scale = 1: 500000
Receiver Height = 1.5 m agl
Frequency = 200.000 MHz
Vertical Polarization

Required Signal Strengths
[redacted]
dB above 1uV/m
Margin is 13.0 dB below

Water

...ations Research Laboratory at the GEC-Marconi Research Centre. (c) GEC-Marconi Ltd. 1990.

COVERAGE PREDICTION 1.4D

Centre = TQ300800
Map is 90.0 km on the side
Scale = 1: 500000
Receiver Height = 1.5 m agl
Frequency = 200.000 MHz
Vertical Polarization

Required Signal Strengths
[redacted]
dB above 1uV/m
Margin is 6.0 dB below

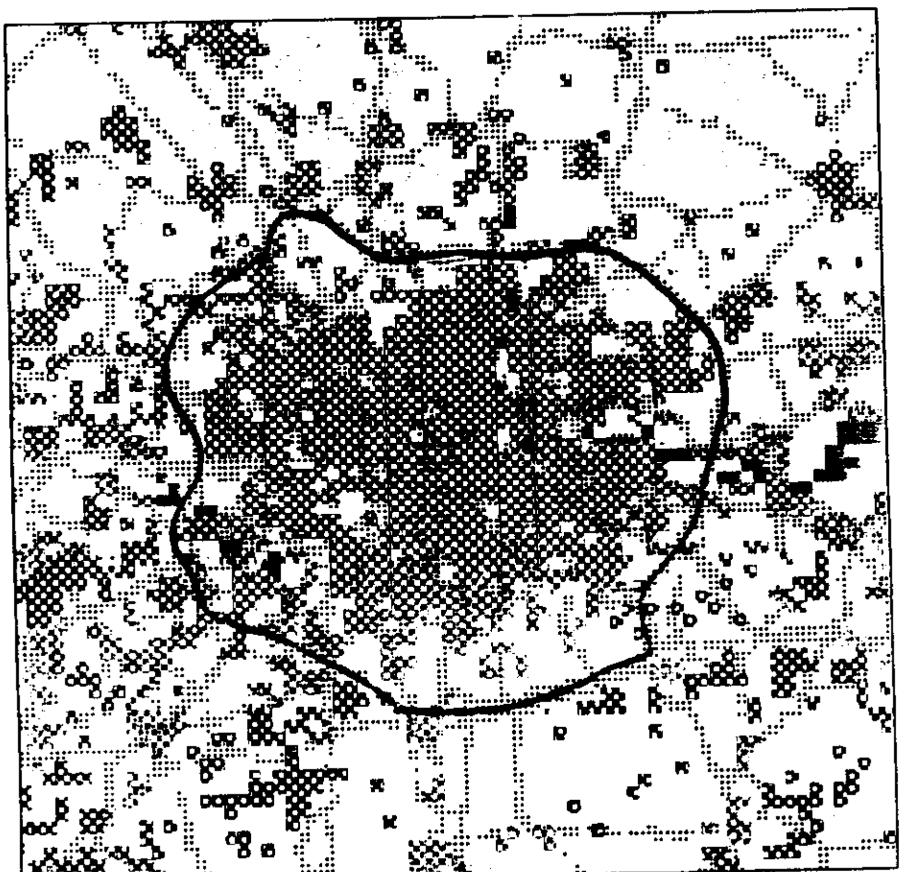

Water
Trees
Roads

PATH PROFILE

Path length

COVERAGE PREDICTION

Centre = TQ300800
Map is 30.0 km on the side
Scale = 1: 500000
Receiver Height = 1.5 m agl
Frequency = 200.000 MHz
Vertical Polarization

Required Signal Strengths

[redacted]

dB above 1uV/m

[redacted]

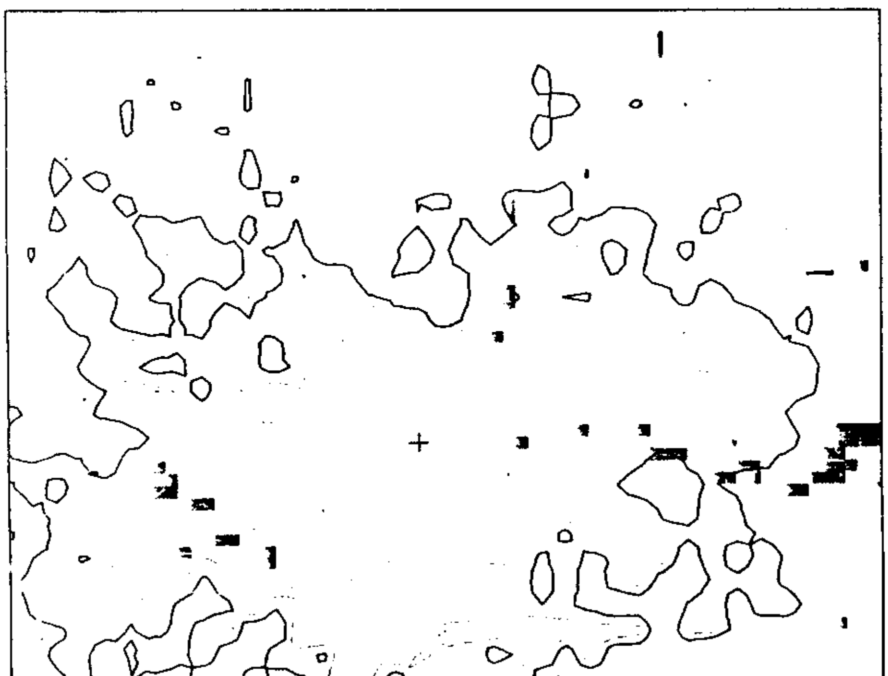

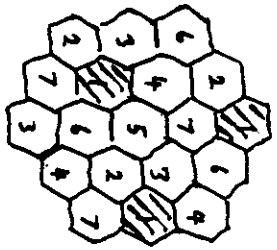

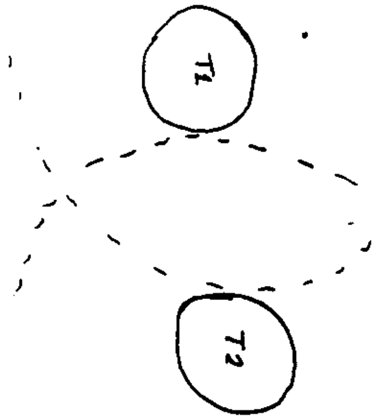

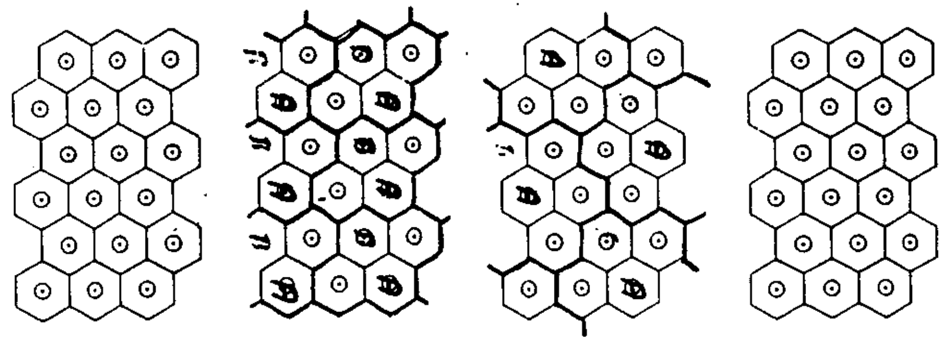

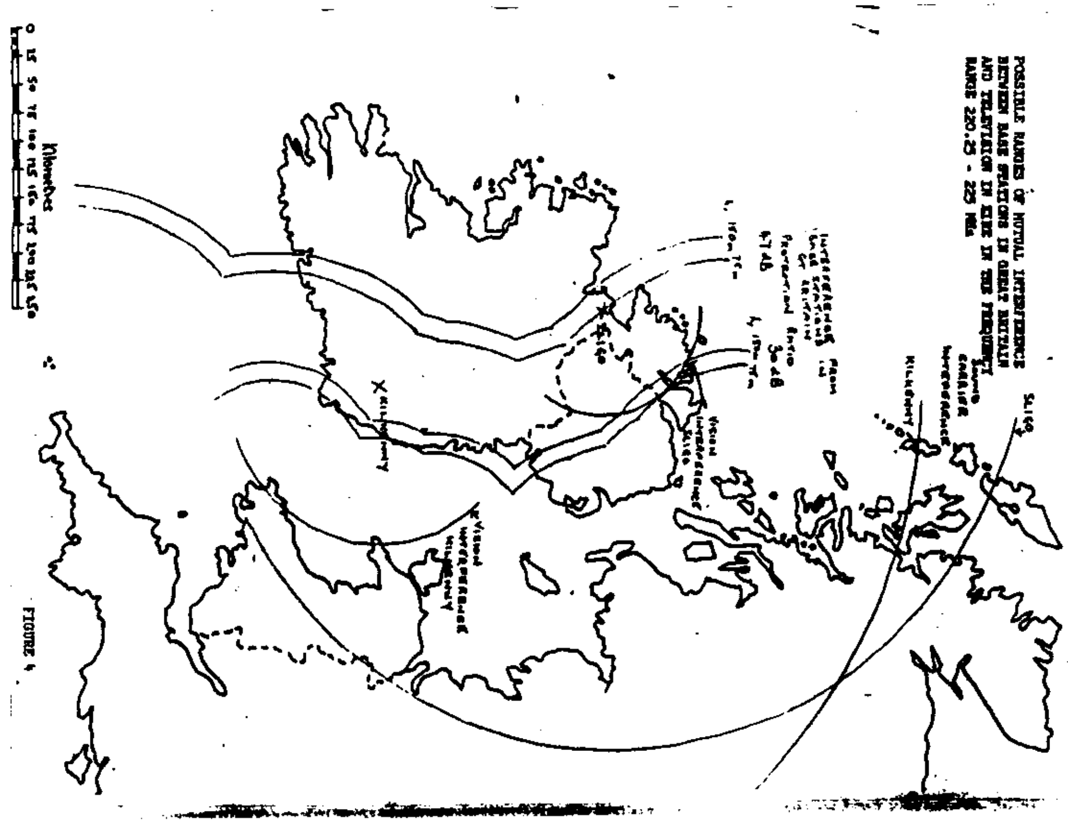

FIGURE 4

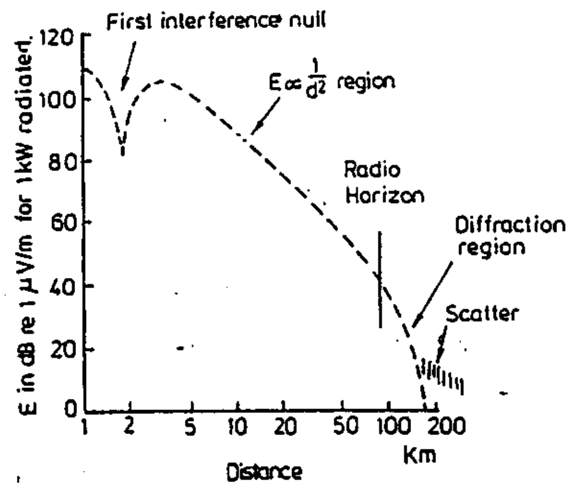

FIGURE 4. Illustrating the different field-strength regimes for propagation between elevated antennas. Horizontal polarization H_t=300 m, h_r=10 m, f=100 MHz.

TROPO-SCATTER

Far into the shadow-zone
- around the bulge of the earth
- signals do not decrease as rapidly

Due to scatter propagation from atmospheric irregularities.

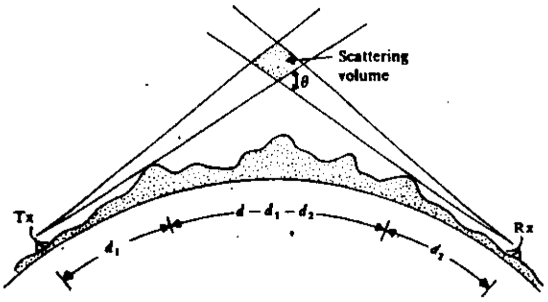

The scatter angle θ of a tropospheric scatter radio link across a mountainous terrain.

The scatter loss, L_{sc}, (as compared with a perfect reflection) is given by (Yeh):

$$L_{sc} = 21 + 0.57\theta + 10 \log f - 0.2(N_s - 310) \text{ dB}$$

mrad (θ) MHz (f)

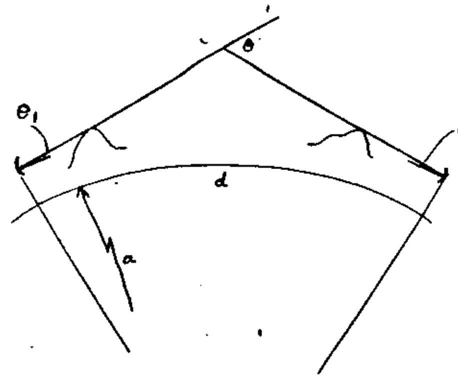

The scatter angle θ is:

$$\theta = \theta_1 + \theta_2 + \frac{d}{10^3 . k a} \text{ mrad}$$

where θ_1 and θ_2 are the horizon clearance angles.

Where the horizon is sea:

$$\theta = \frac{0.157}{k} . d - \frac{0.560}{\sqrt{k}} (\sqrt{h_1} + \sqrt{h_2})$$

The scatter volume is composed of many irregularities, so that a plane wave will not be scattered coherently. This results in a reduction in effective antenna gain, called "aperture to medium coupling loss"

$$L_C = 0.07 \exp\{0.055[G_T + G_R]\} \quad \text{dB}$$

Troposcatter propagation is very variable
- with season
- with climate

Curves giving the difference between worst-month basic transmission loss and annual basic transmission loss

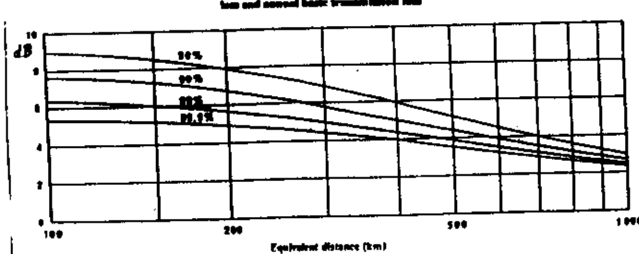

Temperate climate

7-4

Signals also have faster variations:
- log-normally distributed from hour to hour with σ between 3 and 8 dB
- Rayleigh distributed for fast fading.

Since the signal levels are low, this large fading range cannot be coped with.

Diversity is necessary:

space : $\Delta h = (D^2 + 1600)^{1/2}$ m

frequency : $\Delta f = (1.44 f / \theta d)(D^2 + 900)^{1/2}$ MHz

angle : $\Delta \theta_r = \tan^{-1}\left\{\frac{(D^2 + 900)^{1/2}}{500 d}\right\}$

D is the antenna diameter (m)

d is the path length (km)

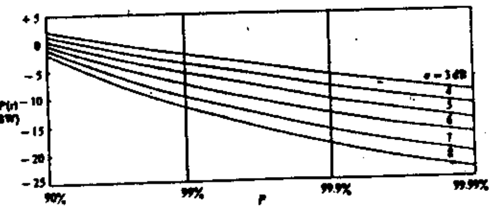

Composite graphs for log-normal slow variation, Rayleigh fast variation and maximal-ratio diversity combining, where σ is the standard deviation associated with the log-normal distribution. The origin refers to the annual median level of $\overline{P(r)}$.